

Broad-band spectroscopy with the James Clerk Maxwell Telescope using a polarizing Fourier transform spectrometer

D. A. Naylor,¹ T. A. Clark,² G. R. Davis,^{3*} W. D. Duncan⁴ and G. J. Tompkins¹

¹*Department of Physics, University of Lethbridge, Lethbridge, Alberta T1K 3M4, Canada*

²*Department of Physics and Astronomy, University of Calgary, Calgary, Alberta T2N 1N4, Canada*

³*Mullard Space Science Laboratory, University College London, Holmbury St Mary, Dorking, Surrey RH5 6NT*

⁴*Joint Astronomy Centre, 660 N. A'ohoku Place, University Park, Hilo, Hawaii 96720, USA*

Accepted 1992 August 12. Received 1992 August 12; in original form 1992 May 18

ABSTRACT

We report the first use of a polarizing Fourier transform spectrometer on the James Clerk Maxwell Telescope. Solar spectra have been measured through four of the submillimetre and millimetre atmospheric windows. The repeatability is shown to be excellent, with signal-to-noise ratios exceeding 100 per spectral element per scan. The spectra also show good agreement with synthetic atmospheric transmission spectra over most of the spectral range. As a demonstration of the potential of this approach for astronomical spectroscopy, the ^{12}CO $J=6-5$ and $7-6$ emission lines from the Orion molecular cloud have been detected for the first time using incoherent techniques.

Key words: atmospheric effects – instrumentation: spectrographs – techniques: spectroscopic – ISM: individual: OMC – ISM: molecules – radio lines: general.

1 INTRODUCTION

Spectral observations through the submillimetre and millimetre atmospheric windows hold promise for many important observations in astronomy, not only for narrow-band line observations using heterodyne detection, but also for broader band, intermediate-resolution spectroscopy using incoherent detection techniques. While the latter approach cannot match the spectral resolution of heterodyne systems, it does offer the ability to measure spectra over a broad spectral range simultaneously and without the necessity for instrument changes and cross-calibration, even in the presence of variable atmospheric conditions. This presents distinct advantages in many astrophysical situations, such as the study of broad spectral features, the measurement of continuum emission, or the search for previously undetected spectral lines.

In 1990 February we explored the feasibility of using an existing classical Michelson interferometer as an intermediate-resolution, broad-band spectrometer for submillimetre astronomy with the James Clerk Maxwell Telescope (JCMT) (Naylor et al. 1991). The atmospheric transmission spectra obtained during this observing run were found to be

in close agreement with a theoretical atmospheric model, and provided the impetus for the development of a polarizing Fourier transform spectrometer (FTS) for use on the JCMT.

In this second paper, we report the first use of a polarizing FTS on the JCMT. During its commissioning run in 1991 February, solar spectra were obtained in the submillimetre and millimetre atmospheric windows under exceptionally dry and stable atmospheric conditions. A selection of these spectra are presented in this paper, from which noise figures for this instrument are derived. The spectra are also compared against synthetic atmospheric transmission spectra in order to assess the influences of the atmosphere and the detector subsystem upon the quality of the data, and to provide a data base for the design of future observing programmes over this wide spectral range.

The commissioning run also produced the first incoherent detections of the ^{12}CO $J=6-5$ and $7-6$ emission lines from the Orion molecular cloud. The results are shown to be in good agreement with previous heterodyne observations, and demonstrate the potential of this technique for astronomical spectroscopy.

2 INSTRUMENTATION AND OBSERVATIONS

The present data were obtained with the polarizing FTS mounted at the east Nasmyth focus of the JCMT, with the bolometric facility detector UKT14 (Duncan et al. 1990)

*Present address: Institute of Space and Atmospheric Studies, University of Saskatchewan, Saskatoon, Saskatchewan S7N 0W0, Canada.

located at its output port. The spectrometer uses a polarizing beamsplitter in conjunction with a polarizer and analyser, each consisting of a 10- μm metal grid on a 2.5- μm Mylar substrate. With the $f/35$ beam of the JCMT Nasmyth focus, the Jacquinot criterion allowed the spectral resolution of 0.0125 cm^{-1} to be obtained without any collimation in the spectrometer.

The polarizing FTS (Martin & Puplett 1970), with the possibility of two input ports and two output ports, offers several significant advantages over the conventional Michelson interferometer which was used in the earlier exploratory work. First, the modulation efficiency of the wire grid beamsplitter is both high and uniform over a wide spectral range, in contrast to the dielectric beamsplitter in which the modulation efficiency exhibits a characteristic lobe pattern. The atmospheric window selected for observation can therefore be changed in a matter of seconds, simply by remotely commanding a filter switch in UKT14. Secondly, the complete separation of radiation from the two input ports alleviates any ambiguity about the source of signal modulation, thereby removing uncertainties in the calibration of the measured spectra. Finally, the optical beamwidths within the present instrument more closely match the JCMT and UKT14 beamwidths and dimensions.

The solar spectra were obtained in two different operating modes. In the ‘rapid scan’ mode, the telescope secondary mirror was held stationary while the moving mirror of the interferometer was scanned through its range of travel in 45 s. Sets of 10 spectra were taken alternately on Sun centre and on a point 2000 arcsec in azimuth from Sun centre (about one solar radius from the Sun’s limb). In the ‘slow scan’ mode, the mirror was continuously scanned at a much slower speed while the telescope secondary mirror was chopped on and off the Sun (close to the limb, by necessity), and the detector output was synchronously rectified to remove remnant atmospheric emission. These scans ranged from 15 to 40 min, depending on frequency, which increased the susceptibility to fluctuations in atmospheric transmission and to occasional transients in the telescope pointing. The resulting data proved to be significantly inferior in quality to those taken in the rapid-scan mode, and have not been included in the present analysis.

In both modes of operation, an ambient-temperature blackbody source was placed in the second input port of the instrument, consisting of a cone fabricated from Eccosorb AN74 (Emerson & Cuming, 604W 182 St, Gardena, CA 90248, USA). Spectra were taken in each of four atmospheric windows, centred on 9, 13, 23 and 29 cm^{-1} . Focal-plane apertures within UKT14 were selected to match the diffraction-limited beamwidth of the telescope for each filter, to provide beams of between 6 and 19 arcsec on the Sun, modified by the significant beam pattern extension detected by solar limb scanning (Lindsey & Roellig 1991; Clark et al. 1992).

Standard Fourier transform spectroscopic analysis techniques were applied to the rapid-scan data. Since the optical elements in the spectrometer and detector produced negligible dispersion over the narrow spectral range of interest, a linear phase correction was determined by weighting phase values obtained from a short double-sided interferogram by the amplitude of the corresponding spectrum, and was applied to each interferogram before Fourier transformation.

3 SOLAR SPECTRA

3.1 Instrument noise characteristics

Representative sets of four individual rapid-scan spectra taken over periods of 6 min are presented for each atmospheric window in Figs 1–4, and demonstrate the excellent repeatability of the instrument over this time interval at all wavelengths. What little variability is present is greater in the higher frequency windows, consistent with the increased sensitivity to fluctuations in atmospheric transmission.

The noise characteristics of the instrument in this configuration have been determined from these data, and are compared in Table 1 to the quoted noise equivalent flux density values for UKT14 when it is used for conventional photometry on the JCMT. The experimental signal-to-noise ratio reaches a limit at the low frequencies as a consequence of inadequate digitization precision used in the data acquisition, a limitation which will be rectified in future measurements. Otherwise, the excellent agreement between these signal-to-noise ratio estimates demonstrates that the extremely small variability in these spectra is entirely attributable to sky noise, in spite of the remarkably dry and stable atmospheric conditions above Mauna Kea during this run.

3.2 Synthetic atmospheric transmission spectra

Synthetic atmospheric transmission spectra have been produced for comparison with the measured solar spectra. These were generated using the multilayer FASCOD2 program (Clough et al. 1981) and the HITRAN data base of spectral line parameters (Rothman et al. 1987). The thermal structure of the atmosphere was represented by the 1976 US Standard Atmosphere applicable to the latitude of these observations. The simulation included the major absorbers H_2O , O_2 and O_3 , as well as the minor absorbers N_2O , CO and CH_4 , although these latter constituents contribute little or no absorption in this spectral region. All absorbers except H_2O were assumed to be invariant with time.

Water vapour is the dominant absorber in this spectral region and is highly variable in both space and time. For the purpose of this simulation, the H_2O column abundance for each scan was determined from measurements of atmospheric opacity at 225 GHz, monitored continuously by the adjacent Caltech Submillimeter Observatory. We used FASCOD, under the same conditions as described above, to determine the form of the dependence of atmospheric opacity at this frequency upon column abundance of H_2O . The result was a linear equation:

$$\tau = 0.0493 w + 0.016,$$

where τ is the zenith opacity at 225 GHz and w is the precipitable water vapour in mm. From the recorded values of the 225-GHz opacity, this relationship was used to determine the column abundance of H_2O for inclusion in the atmospheric simulation, distributed in accordance with the standard atmosphere in this model. In fact, the atmosphere was found to be exceptionally stable throughout these measurements, and was estimated to contain only 0.3 mm of precipitable water vapour for all spectra presented herein.

Also included in this simulation was the empirical H_2O ‘continuum’ absorption which, though poorly defined in the submillimetre region, nevertheless contributes significant

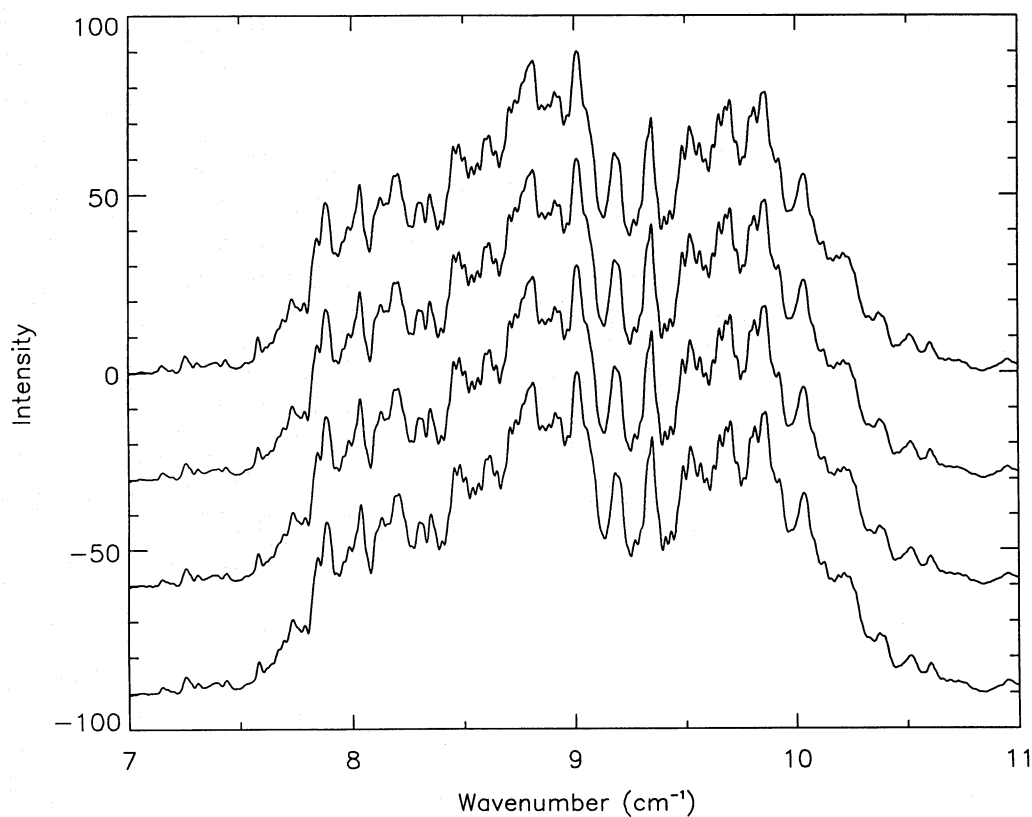


Figure 1. Four individual solar spectra, 7–11 cm^{-1} , taken through 1.75 airmasses.

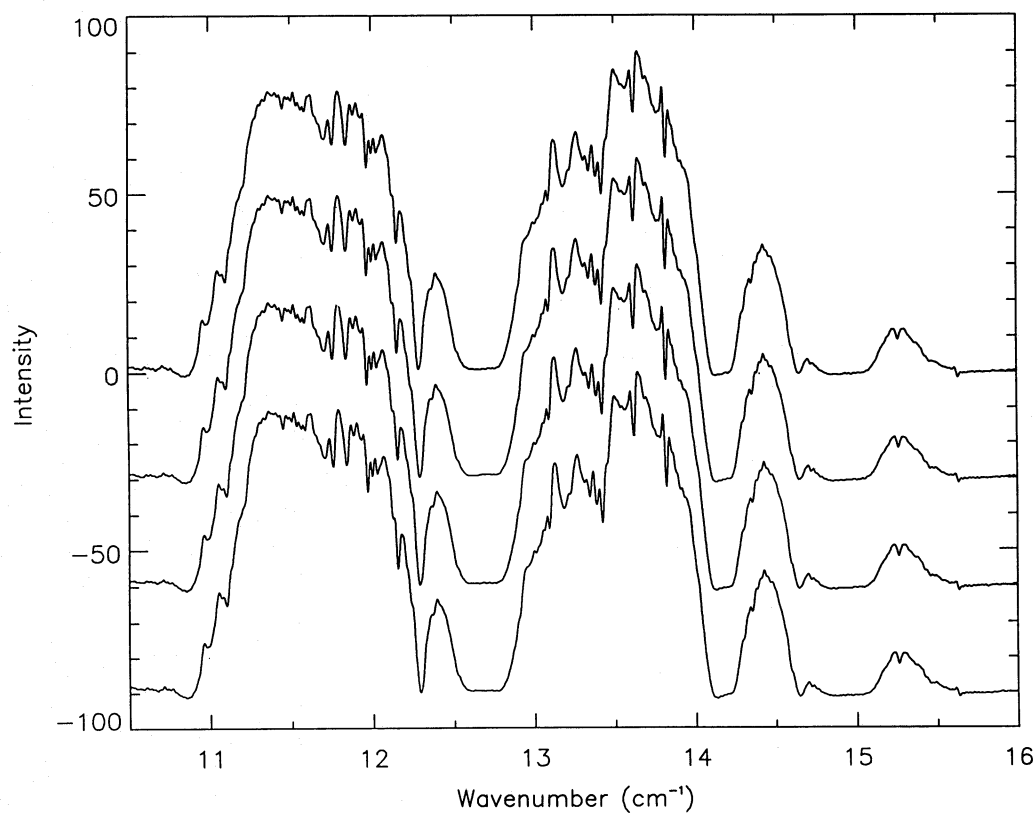


Figure 2. Four individual solar spectra, 10.5–16 cm^{-1} , taken through 3.27 airmasses.

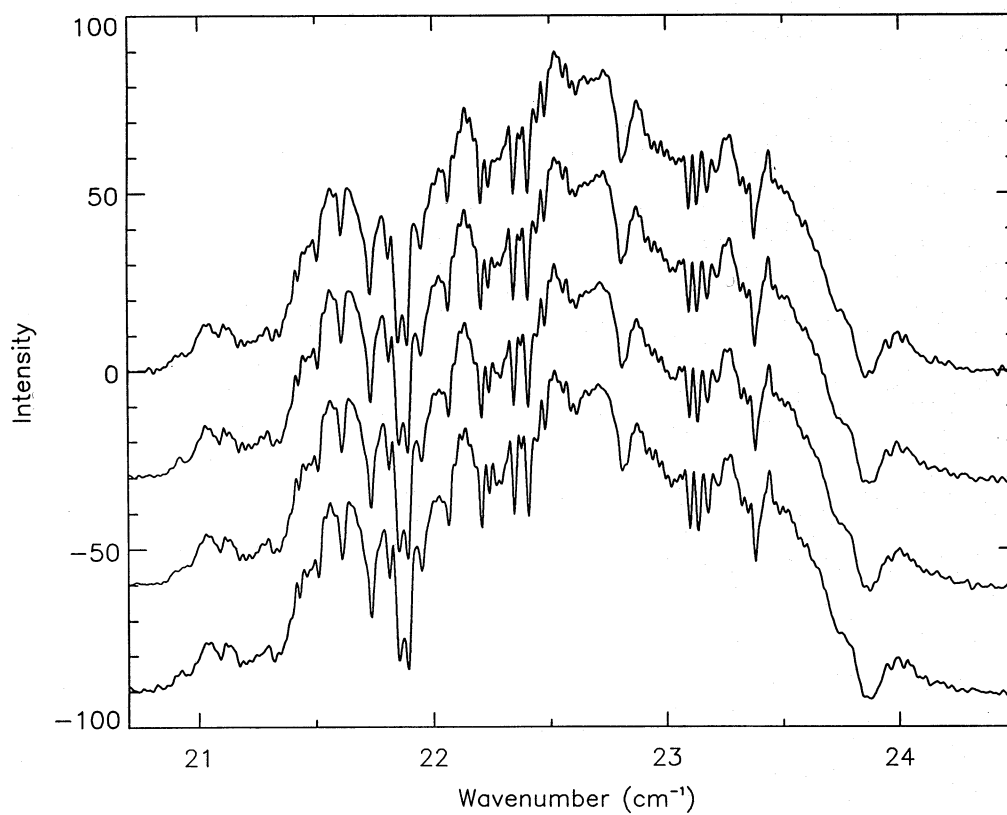


Figure 3. Four individual solar spectra, 20.6–24.5 cm^{-1} , taken through 2.45 airmasses.

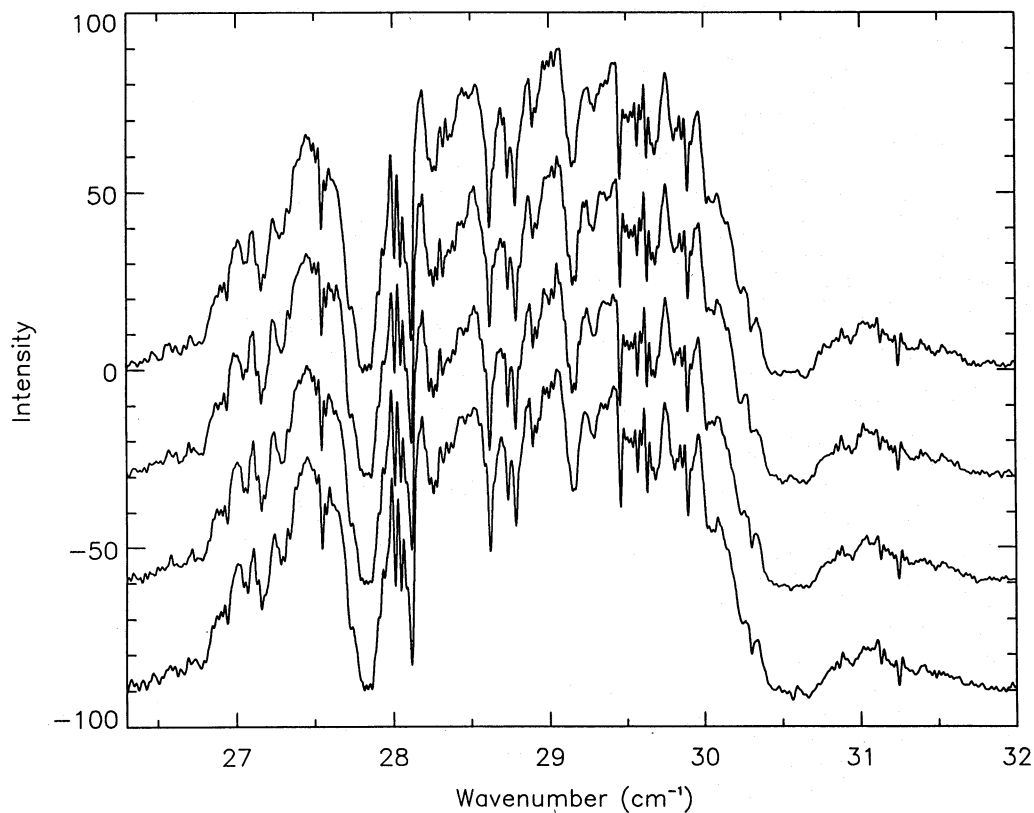


Figure 4. Four individual solar spectra, 26.3–32 cm^{-1} , taken through 2.1 airmasses.

Table 1. Theoretical and experimental noise estimates for the Sun in rapid-scan mode (45 s per interferogram).

Filter /cm ⁻¹	Beam width /arc sec	NEFD Jy/√Hz	Theoretical S/N	Experimental S/N
7-11	19	0.35	6100	750
10.5-16	14	0.5	1800	750
20.7-24.5	7	5	160	150
26.3-32	6	10	75	80

opacity. Despite measurements of this continuum absorption at lower frequencies by Rice & Ade (1979) and at higher frequencies by Davis (1987), it remains a significant source of uncertainty in these calculations. We are therefore engaged in an experiment to measure the atmospheric emission spectrum directly, with the aim of refining the parametrization of the H₂O continuum. The internal FASCOD parametrization was used in the present synthesis.

3.3 Comparison of the spectra

The averages of each set of four rapid-scan spectra from Figs 1-4 are compared, in Figs 5-8, with the corresponding synthetic atmospheric spectra. The synthetic spectra were adjusted to take account of the different airmasses of the measured spectra, and have also been multiplied by the transmissions of the UKT14 filters for direct comparison. Also plotted in these figures are calibration spectra taken with an ambient-temperature blackbody in one port of the instrument and a cooled blackbody (77 K) in the other port.

It is immediately apparent that, in three of the four atmospheric windows (Figs 6-8), the syntheses represent excellent fits to the measured spectra. In the low-frequency window (Fig. 5), however, the measured spectrum is dominated by channel fringes and is more closely matched to the calibration spectrum. These fringes also appear in the other windows, although with smaller amplitude; in addition, although the Moon was poorly placed in the sky for use as an immediate calibration source during this run, lunar spectra taken at much lower airmass and at a different time from the solar data show similar fringing. The channelling is therefore clearly of instrumental origin. Two principal components have been identified, with frequencies of 0.17 and 1 cm⁻¹, and have been attributed to resonant cavities in the detector subsystem: one formed by the two faces of the cryostat window, and the other by the back of the window and the low-pass filter. These will be eliminated in future runs by the use of a wedged window.

4 ORION CO EMISSION LINES

Since the discovery of the high-velocity plateau emission observed in millimetre and microwave lines (Zuckerman & Palmer 1975) and the near-infrared observation of H₂ emission (Gautier et al. 1976), the BN-KL region of the Orion molecular cloud has been extensively studied and modelled in terms of expanding shock waves interacting with the ambient molecular cloud. The best-studied molecule is CO, for which several transitions up to $J=30$ have been observed (Watson et al. 1980). The rotational lines of CO are

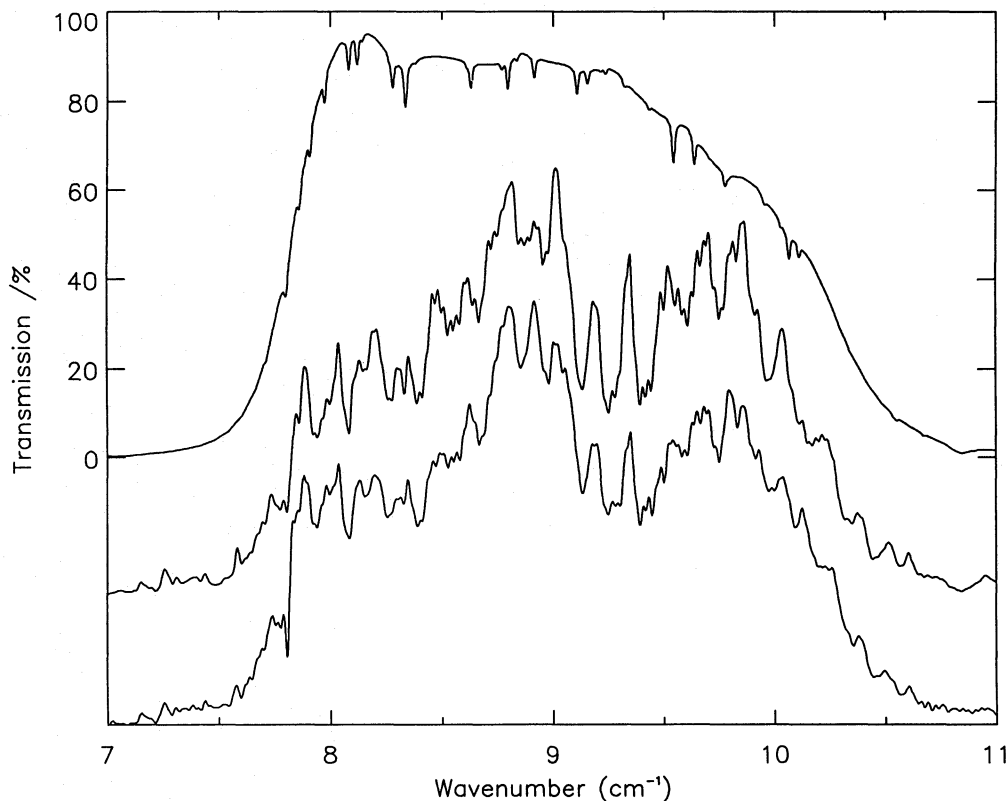


Figure 5. Comparison of spectra, 7-11 cm⁻¹. Top: synthetic atmospheric transmission spectrum; middle: average solar spectrum; bottom: calibration blackbody spectrum.

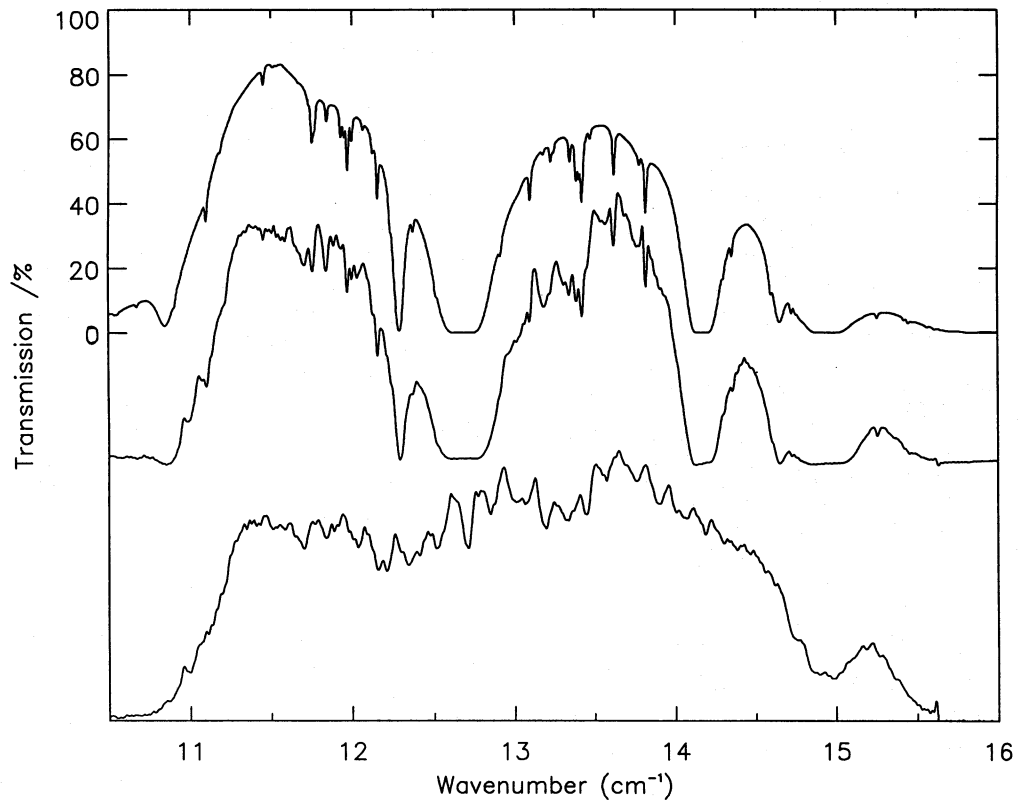


Figure 6. Comparison of spectra, 10.5–16 cm^{-1} . Top: synthetic atmospheric transmission spectrum; middle: average solar spectrum; bottom: calibration blackbody spectrum.

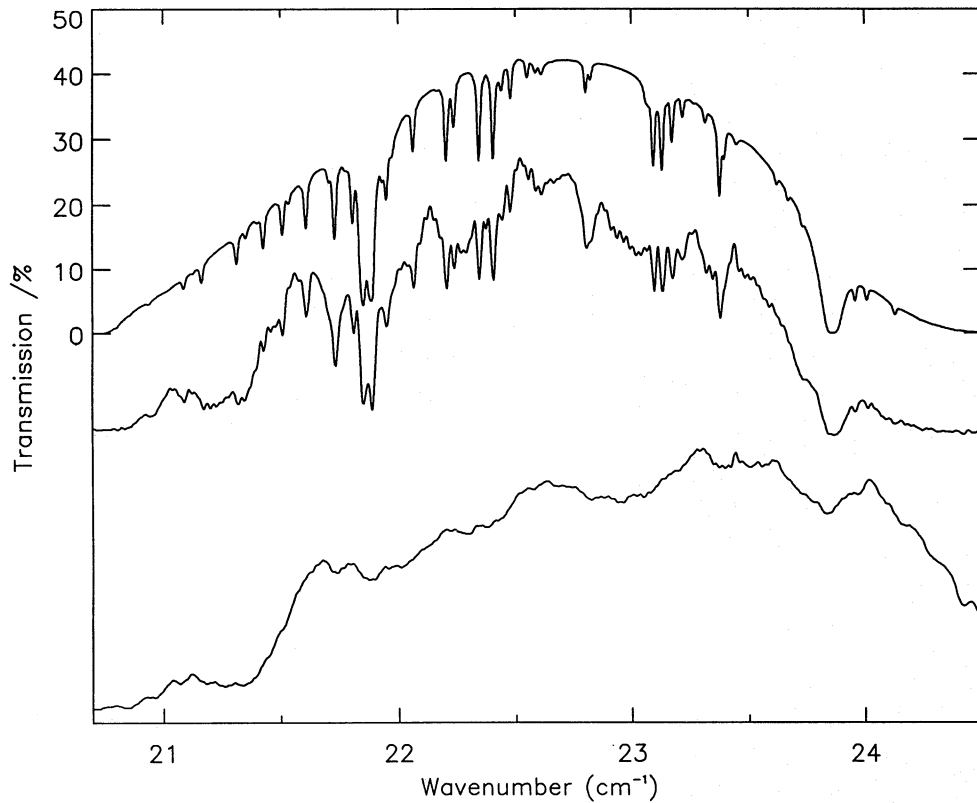


Figure 7. Comparison of spectra, 20.6–24.5 cm^{-1} . Top: synthetic atmospheric transmission spectrum; middle: average solar spectrum; bottom: calibration blackbody spectrum.

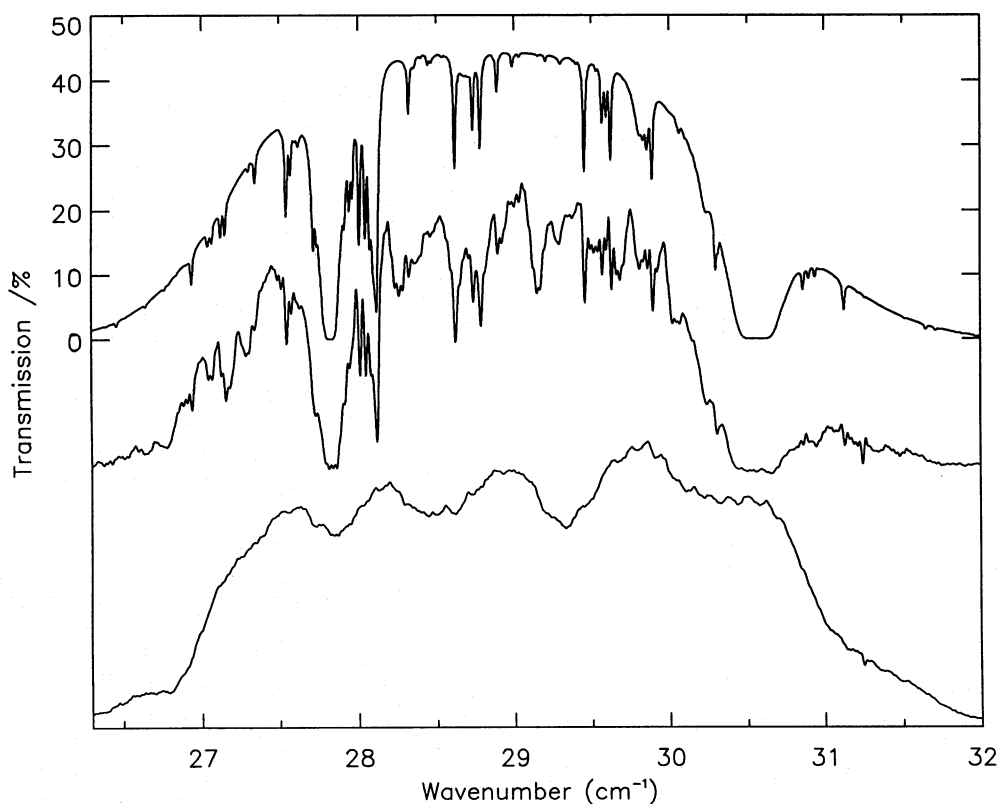


Figure 8. Comparison of spectra, 26.3–32 cm^{-1} . Top: synthetic atmospheric transmission spectrum; middle: average solar spectrum; bottom: calibration blackbody spectrum.

important coolants of the shocked gas (Hollenbach & McKee 1979) and their measurement serves as a useful probe of the physical conditions of such regions.

Since the $^{12}\text{CO } J=6-5$ and $7-6$ transitions fall in the submillimetre windows used in this commissioning run of the polarizing FTS, one interferogram of the Orion molecular cloud core was obtained for each window. The spectrometer was operated in slow-scan mode for these measurements. Previous observations of these lines have employed heterodyne spectrometers. The first detection of the $^{12}\text{CO } J=6-5$ line in Orion (Goldsmith et al. 1981) found a hot (~ 100 K) and relatively broad ($\Delta v = 26 \text{ km s}^{-1}$) feature readily identified with the plateau source. The $^{12}\text{CO } J=7-6$ line was subsequently detected by Schultz et al. (1985) and was found to have similar parameters (~ 110 K, $\Delta v = 35 \text{ km s}^{-1}$).

Fig. 9 shows the $^{12}\text{CO } J=6-5$ line at 23.0651 cm^{-1} detected with the present instrument towards Orion IRC2 on 1991 February 26. The spectrum is unapodized with a resolution of 0.0125 cm^{-1} (165 km s^{-1}), and exhibits the classical sinc-function line profile of an ideal interferometer. The baseline ripple seen in this spectrum is a result of channel fringing, as discussed above. The line position, as determined from fitting to the profile, is 23.065 cm^{-1} . While the intensity scale of Fig. 9 is arbitrary, the peak temperature of the CO line has been estimated from comparison with a spectrum of Mars obtained some 4 h earlier. Since the atmosphere was exceptionally transparent and stable during this period, it was possible to calibrate the Orion spectrum by combining the difference in airmass of the Mars and Orion observations with the extinction coefficient for the line

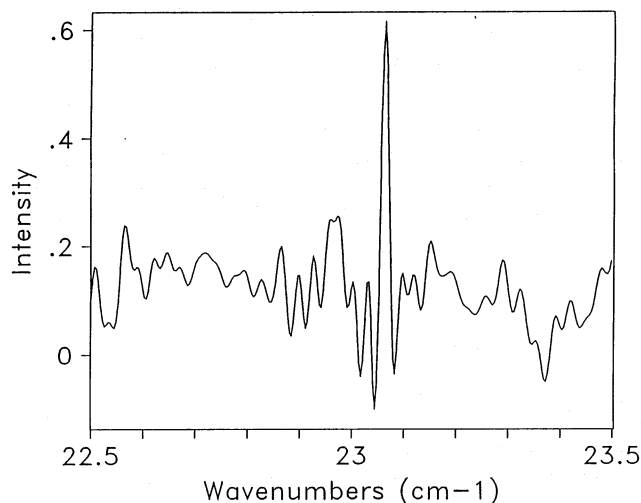


Figure 9. The $^{12}\text{CO } J=6-5$ line at 23.0651 cm^{-1} detected toward Orion IRC2 ($5^{\text{h}}32^{\text{m}}47^{\text{s}}$, $-5^{\circ}24'23''$). The spectral resolution is 0.0125 cm^{-1} or 165 km s^{-1} ; the intensity scale is arbitrary.

frequency as determined from synthetic modelling. The effects of beam dilution and the assumed continuum Martian temperature have been accounted for in this analysis. With these assumptions, the peak temperature of the CO line is determined to be 36 K. While it is not possible to place an error on this temperature, since only one spectrum of Orion was obtained, it is nevertheless instructive to calculate the expected temperature in a 165 km s^{-1} resolution element

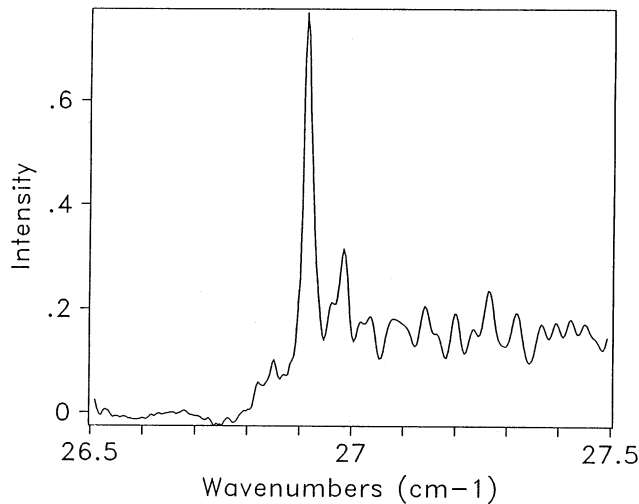


Figure 10. The $^{12}\text{CO } J=7-6$ line at 26.9070 cm^{-1} detected toward Orion IRc2 ($5^{\text{h}}32^{\text{m}}47^{\text{s}}$, $-5^{\circ}24'23''$). The spectral resolution is 0.0125 cm^{-1} or 140 km s^{-1} ; the intensity scale is arbitrary.

from the recent heterodyne measurements of Graf et al. (1990). These authors determine the line parameters to be $T=133 \text{ K}$ and $\Delta v=44.2 \text{ km s}^{-1}$, which is equivalent to a temperature of 35.6 K in one resolution element of the Fourier spectrometer, in excellent agreement with that observed.

Fig. 10 shows the $^{12}\text{CO } J=7-6$ line at 26.9070 cm^{-1} from Orion IRc2, measured just prior to the $J=6-5$ observation. Since this line falls on the steep edge of the UKT14 filter used in these observations, intensity calibration has proven difficult. The filter cuts on at 26.8 cm^{-1} (Fig. 10), and has a transmission of only ~ 20 per cent at the line position. The position of the line as determined from fitting to the profile is 26.912 cm^{-1} , in close agreement with theory. Given the uncertainties in the calibration, the effective temperature of the line, as determined from a Mars spectrum, is around 40 K , which is consistent with the $^{12}\text{CO } J=6-5$ result when account is taken of the increased spectral resolution at this frequency (140 km s^{-1}).

5 CONCLUSIONS

A polarizing FTS has been used for the first time on the JCMT, in conjunction with the facility bolometric detector UKT14. The solar spectra presented herein demonstrate significant improvement in spectral quality and reproducibility over those measured in 1990 with a classical Michelson interferometer (Naylor et al. 1991). Two CO emission lines from the Orion molecular cloud have been measured, and are in good agreement with heterodyne observations.

Use of polarization encoding has enabled us to extend the spectral range to include all of the submillimetre and millimetre atmospheric windows from 7 to 30 cm^{-1} . The ability to configure the spectrometer to observe in any of the UKT14 filter bands in just a few seconds provides high operating efficiency and removes the need for complex cross-calibration, since observations are conducted with essentially the same telescope and instrument parameters and under the same atmospheric conditions.

While Fourier spectrometers have intrinsically lower spectral resolution than heterodyne receivers, they are ideally suited to astrophysical applications which require broad spectral coverage and simultaneous measurement of the continuum. Examples include pressure-broadened absorption lines of constituents in planetary atmospheres, the search for and identification of spectral features in planetary atmospheres and molecular clouds, and broad-line emission from extragalactic sources.

Encouraged by the present results, we intend to increase the resolution of the polarizing spectrometer by a factor of ~ 3 . Based on the results presented in this paper and a detailed analysis of the spectrometer performance, we anticipate that it will be possible to measure line intensities with an accuracy of $< 0.5 \text{ K}$ in resolution intervals of $\sim 50 \text{ km s}^{-1}$ within a few minutes under reasonable atmospheric conditions on the JCMT.

ACKNOWLEDGMENTS

The James Clerk Maxwell Telescope is operated by the Royal Observatory Edinburgh on behalf of the UK Science and Engineering Research Council (SERC), the Netherlands Organization for Scientific Research (NWO) and the Canadian National Research Council. The authors wish to thank Dr P. A. R. Ade of Queen Mary and Westfield College, London, for providing the polarizers and roof-top mirrors used in the interferometer, and without whose support these experiments would have been impossible. It is also a pleasure to acknowledge the staff of the JCMT who readily assisted in the mounting of the interferometer at the Nasymth focus of the telescope and provided excellent support during the run. This research was funded in part by grants from NSERC and NRC, Canada (DAN and TAC), and from SERC, UK (GRD).

REFERENCES

- Clark T. A., Naylor D. A., Tompkins G. J., Duncan W. D., 1992, *Solar Phys.*, 140, 393
- Clough S. A., Kneisys F. X., Rothman L. S., Gallery W. O., 1981, *Proc. SPIE*, 277, 152
- Davis G. R., 1987, DPhil thesis, University of Oxford
- Duncan W. D., Robson E. I., Ade P. A. R., Griffin M. J., Sandell G., 1990, *MNRAS*, 243, 126
- Gautier T. N., Fink U., Treffers R. P., Larson H. P., 1976, *ApJ*, 207, L129
- Goldsmith P. F. et al., 1981, *ApJ*, 243, L79
- Graf U. U., Genzel R., Harris A. I., Hills R. E., Russell A. P. G., Stutzki J., 1990, *ApJ*, 358, L49
- Hollenbach D. J., McKee C. F., 1979, *ApJS*, 41, 555
- Lindsey C. A., Roellig T. L., 1991, *ApJ*, 375, 414
- Martin D. H., Puppelt E. F., 1970, *Infrared Phys.*, 10, 105
- Naylor D. A., Clark T. A., Schultz A. A., Davis G. R., 1991, *MNRAS*, 251, 199
- Rice D. P., Ade P. A. R., 1979, *Infrared Phys.*, 19, 575
- Rothman L. S. et al., 1987, *Appl. Opt.*, 26, 4058
- Schultz G. V., Durwen E. J., Roser H. P., Sherwood W. A., Wattenbach R., 1985, *ApJ*, 291, L59
- Watson D. M., Storey J. W. V., Townes C. H., Haller E. E., Hansen W. L., 1980, *ApJ*, 239, L129
- Zuckerman B., Palmer P., 1975, *ApJ*, 199, L35